Photoemission induced bias in two-dimensional silicon pn junctions

M. Lavayssière,[1] O. Renault,[1] D. Mariolle,[1] M. Veillerot,[1] J. P. Barnes,[1] J. M. Hartmann,[1] J. Leroy,[2] and N. Barrett[2,a)]
[1]*CEA, LETI, Minatec Campus, F-38054 Grenoble Cedex 09, France*
[2]*CEA, IRAMIS, SPCSI, LENSIS, F-91191 Gif-sur-Yvette, France*

(Received 10 September 2011; accepted 31 October 2011; published online 16 November 2011)

Spectroscopic x-ray photoelectron emission microscopy was used to study the role of the pn junction on imaging of micron scale n- and p-doped silicon patterns epitaxially grown on p- and n-type substrates, respectively. In the closed n-doped patterns, contrast with respect to open patterns is observed in both work function and Si 2p binding energy. Reverse bias at the junction creates a shift of electrical potential induced by photoemission in the closed patterns. No shift is observed for p-doped patterns on n substrate, pointing to the importance of doping combination and pattern geometry in the contrast observed in electron microscopy. © *2011 American Institute of Physics*. [doi:10.1063/1.3662440]

Semiconductor doping contrast in electron microscopy attracts much interest due to the need of the microelectronic industry for direct, reliable methods to determine doping at various scales in devices. The first observation of such contrast with brighter p regions than n ones used secondary electrons in a scanning electron microscope (SEM),[1] confirmed by photoelectron emission microscopy (PEEM),[2,3] and low-voltage SEM.[3] The intensity measured from p and n type regions has been interpreted in terms of band bending[2,4] with additional factors arising from detection geometry.[5] However, imaging of finite sized, two-dimensional domains, relevant for device applications, has yet to be fully studied. Hovorka *et al.*[6] observed some fascinating three-level contrast on small p-type doped patterns implanted into a n-type substrate using high-pass energy filtered PEEM. Spectroscopic PEEM is particularly powerful since it combines high spatial and energy resolution, allowing a comprehensive analysis of doped regions using secondary and core level electrons.[7] We present a spectroscopic x-ray excited PEEM (XPEEM) study of the role of the pn junction on imaging of micron scale, epitaxial n- and p-doped silicon patterns on p- and n-type substrates, respectively. Spatially resolved work function and Si 2p core level binding energies are consistent with an overall rigid shift in n-doped windows on a p type substrate. SEM, Kelvin force microscopy (KFM), scanning capacitance microscopy (SCM), and focused ion beam (FIB) confirm that the n-type regions are at a different electrical potential when fully enclosed by a p-type substrate. Two samples were prepared, highly n-doped patterns on a p-doped substrate and highly p-doped patterns on a n-doped substrate, hereafter referred to as N^+/P and P^+/N. The underlying substrate in both cases was p-doped Si(100) (resistivity 5–10 Ω cm). To obtain a n-type substrate, a 150 nm thick n-type epitaxial blanket layer was grown at the beginning of the process. A SiO_2 hard mask and deep-UV photolithography with anisotropic etching were used to define patterns. HF-last wet cleaning followed by an *in-situ* H_2 bake at 950 °C removed the native oxide. 100 nm cavities were etched using gaseous HCl (180 Torr, 750 °C), then *in-situ* selective epitaxial growth of boron and phosphorous doped silicon in the cavities was carried out at 950 °C, 20 Torr using SiH_2Cl_2, B_2H_6, and PH_3 gaseous precursors (as for embedded SiGe sources and drains[8]). Epitaxial growth was preferred to avoid damage due to the implanted ion energy and to obtain more abrupt pn junctions. The doping precursors were diluted in H_2.[9] Finally, the SiO_2 hard mask was removed with HF. For each sample, two patterns were obtained: closed, inside the zero, and open, outside the zero, as shown in the atomic force microscopy (AFM) image (Fig. 1).

The doping levels were checked with dual-beam time-of-flight secondary ion mass spectrometry using 1 keV O_2^+ (Cs^+) sputtering for the boron (phosphorous) and with SCM. N^+ and P^+ patterns had doping levels of 1.8 and 1.0×10^{19}atoms cm^{-3}, respectively. The *N* substrate doping was 5.4×10^{17}atoms cm^{-3}. Topography was measured by AFM (Fig. 1). The pattern was 20 nm (50 nm) lower than the surrounding substrate for N^+/P (P^+/N) samples. Given the large pattern dimensions (10 μm), the height differences are only expected to influence imaging near the pn junction.[10] The surfaces were passivated using a three step process to reduce band bending. After degreasing in trichloroethylene, rinsing in acetone and de-ionized water, a first etching was done using a buffered oxide etchant (BOE: 49% HF, 40% NH_4 F in a 7:1 ratio). The sample was then chemically oxidized using a Piranha solution (1/3 H_2O_2, 2/3 H_2SO_4, concentrations 30% and 96%, respectively) for 20 min. The

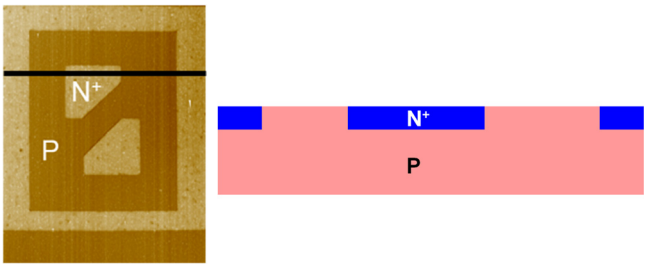

FIG. 1. (Color online) (left) AFM topography of N^+/P, z-scale 30 nm. (right) Profile of the sample along black line.

a)Author to whom correspondence should be addressed. Electronic mail: nick.barrett@cea.fr.

sample was re-etched in BOE for 30 min, dried under N_2, and immediately introduced into the XPEEM vacuum system. Fourier transform infra-red spectroscopy in attenuated total reflectance mode and angle-resolved XPS (not shown) confirmed that the passivation had largely removed the native oxide with Si-H, the dominant surface bond. The experiments were performed using an energy-filtered XPEEM (NanoESCA, Omicron Nanotechnology)[11] on the TEMPO beamline of the SOLEIL synchrotron ($h\nu = 128.9$ eV). The depth sensitivity of the Si 2p level was 2.3 nm. The extractor voltage was 12 kV, the contrast aperture 70 μm, and the field of view (FoV) 62 μm. The analyzer slit was set to 1 mm and the pass energy 50 eV. The overall energy resolution including the photon band width was 0.2 eV, as measured at the Fermi level of a clean, single crystal Ag sample, also used to calibrate the binding energy (BE). Threshold and core level image series were acquired as a function of photoelectron kinetic energy referenced to the sample Fermi level. The threshold directly measures the sample work function. Dark field and flat field imaging eliminated camera noise and detector inhomogeneity, respectively, and the non-isochromaticity was corrected.[11,12] Pixel-by-pixel spectra were extracted using a customized MATLAB routine. Complementary measurements were carried out using SCM and KFM to measure the doping levels and the surface potential.

The threshold spectra were fitted using a complementary error function, providing a 2D work function map (Fig. 2(a)) with a standard deviation of ± 0.02 eV. The values obtained are given in Table I. In the N^+/P sample, the closed N^+ patterns have a work function 0.21 eV higher than the open ones, whereas in the P^+/N sample they are identical. Surface

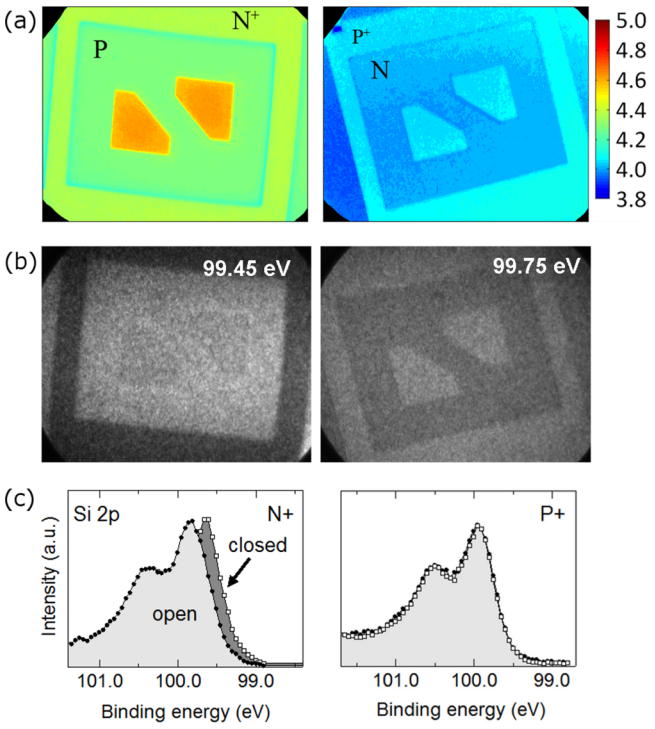

FIG. 2. (Color online) (a) Work function maps from threshold PEEM. (b) SR Si 2p images of highly doped patterns at the half maximum of the low BE side. (c) Si 2p spectra of heavily doped patterns; the closed pattern is dark gray and the open region is light gray. In each case, N^+/P (left) and P^+/N (right).

TABLE I. PEEM work function and Si^0 2p core level binding energy for N^+ and P^+/N samples, with KFM work function for N^+/P measured in air. Open and closed regions are denoted (o) and (c).

	N^+ (c)	N^+ (o)	P^+ (c,o)
PEEM Φ_{WF} (eV)	4.65 ± 0.01	4.44 ± 0.01	4.19 ± 0.022
Si 2p BE (eV)	99.64 ± 0.05	99.77 ± 0.05	99.89 ± 0.05
KFM Φ_{WF} (eV)	4.85 ± 0.05	4.70 ± 0.05	—

photo-voltage could modify the band bending due to residual oxide at the surface,[13–15] but XPEEM using a laboratory Al Kα source with a much lower flux confirmed the synchrotron radiation (SR) results. Fig. 2(b) shows representative images taken at equivalent positions in the Si 2p spectra (low BE edge of the Si^0 part of the spectrum). The triple contrast is obvious in the case of the N^+/P sample, whereas the P^+/N sample shows only contrast between the N doped substrate and the P^+ patterns, whether open or closed. Fig. 2(c) shows the Si 2p micro-spectra obtained for the open and closed doped regions. In the case of the N^+/P sample, the Si^0 peak in the closed N^+ region has a lower BE than in the open N^+ region. Together with the work function shift, they point conclusively to an overall rigid shift of the Si bands. The core level spectra were fitted using standard parameters from literature.[12,16] The detailed analysis will be reported elsewhere; here, we focus on the Si^0 component, indicative of the band alignment in each region. The results are given in Table I. In the N^+ sample, the Si^0 peak is shifted 0.13 eV to lower binding energy in the closed zone, whereas for the P^+/N sample, the Si^0 peak in the P^+ region is the same in both the closed and open regions. The values of the Si^0 binding energies and work function do not correspond to the flat band values expected from the doping levels. This is because the probing depth of 2.3 nm using SR is comparable to the depletion width. The values obtained will thus reflect the band bending at the surface. Also, despite passivation protocol, there is a small residual oxide, less than 1 nm thick which will bend the surface bands. The SEM image of the N^+/P sample in Fig. 3(a) shows clear contrast between the closed and open regions which is attenuated with increasing through lens detector voltage and disappears for detector voltages greater than 50 V (not shown). FIB with a primary beam radiation of 30 keV Ga^+ ions also gave enhanced secondary electron emission (not shown) in closed N^+ regions. Fig. 3(b) shows the relative surface potential as measured by KFM. The open N^+ region has a work function 0.15 eV lower than the closed one. Assuming a tip work function of 5.1 eV, we obtain 4.85(4.7) eV for the closed (open) pattern. The difference with respect to the PEEM result can be explained by the fact that the adsorbate sensitive KFM is done in air. SCM confirmed that the doping levels in the closed and open area were the same. The energy shift cannot be related to the residual oxide layer since the core level spectra show no significant intensity difference between the patterns. Photon, electron, and primary ion excitation give similar results, suggesting that the appearance of triple contrast is due to the sample itself. In the XPEEM experiment, the sample is referenced to ground. A sufficiently conducting sample will not show charging effects often associated with

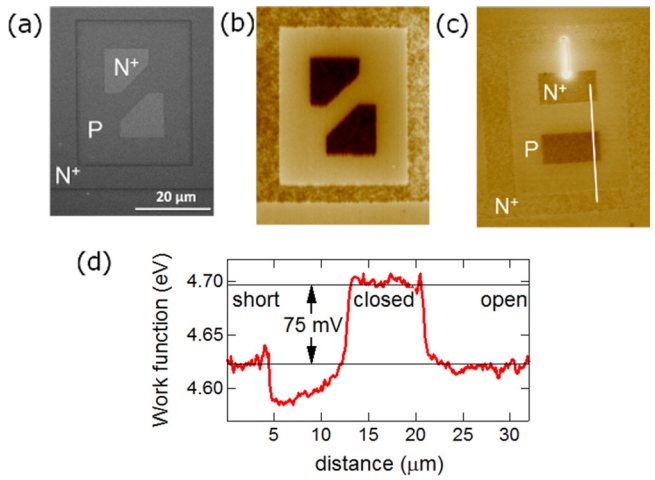

FIG. 3. (Color online) (a) SEM (2 keV, 0.2 nA) image of N^+/P sample. (b) KFM surface potential image of same assuming tip work function of 5.1 eV. (c) KFM surface potential image obtained after short circuiting the closed and open N^+ regions using FIB and (d) profile along the white line in (c).

photoemission from insulating samples. The photon beam is larger (100 μm) than the FoV. However, the closed pattern of the N^+/P sample is surrounded by a pn junction, whereas the P substrate is directly connected to ground. Photoemission will polarize the closed N^+ patterns positively with respect to the P substrate, inducing a reverse bias across the junction, preventing electrons from the substrate from screening the photo-holes. Thus, a potential difference is created between the closed and open patterns, shifting the measured electron energies. The open N^+ patterns are grounded via the top of the sample holder allowing screening of the core holes. In the case of the P^+/N sample, neither the closed P^+ nor the surrounding N regions are directly grounded since the latter is a blanket on a P type substrate, but only 50 nm of depleted N silicon separates the P^+ from the P substrate, thus there is an effective forward bias across the junction allowing charge compensation. The observed shifts are a direct result of the photo-induced bias condition which depends on the sample doping configuration. To check the existence of reverse bias under photoemission, we have created a 50 nm conducting channel between the closed and open N^+ patterns using FIB milling followed by electron beam induced deposition of a tungsten strap. Fig. 3(c) shows that the closed pattern shorted to the open pattern has indeed a different surface potential compared with the other closed N^+ pattern, isolated by its all-round pn junction. The metallic short is bright because of its lower work function but far from it, the modified surface potential of the pattern can be measured. The work function of the short-circuited N^+ pattern is the same as that of the open pattern and both are 75 mV lower than that of the unshorted closed pattern. The difference with respect to the KFM results of Table I may be due to slight surface alteration during the FIB/SEM step. We have used high-transmission energy filtered XPEEM to measure photoemission induced bias in two-dimensional silicon pn junctions. Closed patterns, fully surrounded by a pn junction can show an unusual triple contrast behavior, which is not due to surface chemistry or variations in the doping levels. In the case of highly n-doped patterns on a p type substrate, photoemission induces a reverse bias at the pn junction preventing screening of the core-holes, resulting in a rigid shift of the Si bands. Thus, infinite, doped patterns, photoemission induced bias can influence imaging contrast and may have interesting applications in the field of light sensors.

M.L. benefited from a CEA Ph.D. grant. The work was supported by the French National Research Agency (ANR) Recherche Technologique de Base (RTB) program. We thank SOLEIL for provision of SR facilities and the TEMPO staff for their help.

[1]T. H. P. Chang and W. C. Nixon, Solid-State Electron. **10**, 701 (1967).
[2]V. W. Ballarotto, K. Siegrist, R. J. Phaneuf, and E. D. Williams, J. Appl. Phys. **91**, 469 (2002).
[3]L. Frank, F. Mika, M. Hovorka, D. Valdaitsev, G. Schönhense, and I. Müllerová, Mater. Trans. **48**, 936 (2007).
[4]I. Volotsenko, M. Molotskii, Z. Barkay, J. Marczewski, P. Grabiec, B. Jaroszewicz, G. Meshulam, E. Grunbaum, and Y. Rosenwaks, J. Appl. Phys. **107**, 014510 (2010).
[5]J. Cazaux, Ultramicroscopy **107**, 242 (2010).
[6]M. Hovorka, L. Frank, D. Valdaitsev, S. A. Nepijko, H. S. Elmers, and G. Schönhense, J. Microscopy **230**, 42 (2008).
[7]R. J. Phaneuf, H.-C. Kan, M. Marsi, L. Gregoratti, S. Günther, and M. Kiskinova, J. Appl. Phys. **88**, 863 (2000).
[8]D. Cooper, A. Bch, J. M. Hartmann, V. Carron, and J. L. Rouvière, Semicond. Sci. Technol. **25**, 095012 (2010).
[9]F. Gonzatti, J. M. Hartmann, and K. Yckache, ECS Trans. **16**, 485 (2008).
[10]S. A. Nepijko, N. N. Sedov, G. Schönhense, M. Escher, X. Bao, and W. Huang, Ann. Phys. **9**, 441 (2000).
[11]M. Escher, K. Winkler, O. Renault, and N. Barrett, J. Electron Spectrosc. Relat. Phenom. **178–179**, 303 (2010).
[12]F. de la Peña, N. Barrett, L. F. Zagonel, M. Walls, and O. Renault, Surf. Sci. **604**, 1628 (2010).
[13]M. Alonso, R. Cimino, and K. Horn, Phys. Rev. Lett. **64**, 1947 (1990).
[14]M. H. Hecht, Phys. Rev. B **41**, 7918 (1990).
[15]N. Barrett, L. F. Zagonel, O. Renault, and A. Bailly, J. Phys.: Condens. Matter **21**, 314015 (2009).
[16]F. J. Himpsel, F. R. McFeely, A. Taleb-Ibrahimi, J. A. Yarmoff, and G. Hollinger, Phys. Rev. B **38**, 6084 (1988).